Statistical Textural Distinctiveness in Multi-Parametric Prostate MRI for Suspicious Region Detection

Audrey G. Chung*, Christian Scharfenberger, Farzad Khalvati, Alexander Wong, and Masoom A. Haider

Department of Systems Design Engineering,
University of Waterloo,
200 University Ave W, Waterloo, Canada
agchung@uwaterloo.ca

Abstract. Prostate cancer is the most diagnosed form of cancer, but survival rates are relatively high with sufficiently early diagnosis. Current computer-aided image-based cancer detection methods face notable challenges include noise in MRI images, variability between different MRI modalities, weak contrast, and non-homogeneous texture patterns, making it difficult for diagnosticians to identify tumour candidates. We propose a novel saliency-based method for identifying suspicious regions in multi-parametric MR prostate images based on statistical texture distinctiveness. In this approach, a sparse texture model is learned via expectation maximization from features derived from multi-parametric MR prostate images, and the statistical texture distinctiveness-based saliency based on this model is used to identify suspicious regions. The proposed method was evaluated using real clinical prostate MRI data, and results demonstrate a clear improvement in suspicious region detection relative to the state-of-art method.

Keywords: Computer-aided prostate cancer detection, multi-parametric magnetic resonance imaging (MP-MRI), texture-based saliency, statistical textural distinctiveness

1 Introduction

Prostate cancer is the most commonly diagnosed cancer in Canadian men (excluding non-melanoma skin cancers), with an estimated 23,600 new cases and 4,000 deaths from it in 2014 [5]. According to the Canadian Cancer Society, prostate cancer is the third leading cause of death from cancer, accounting for 10% of cancer deaths in Canadian men. Despite these statistics, survival rates are relatively high with sufficiently early diagnosis, making the need for fast and reliable detection methods crucial.

The current clinical model uses a digital rectal exam (DRE) or a prostate-specific antigen (PSA) test for initial screening. Men with a positive DRE or

* This research was undertaken, in part, thanks to funding from the Canada Research Chairs program. The study was also funded by the Natural Sciences and Engineering Research Council (NSERC) of Canada and the Ontario Ministry of Economic Development and Innovation.

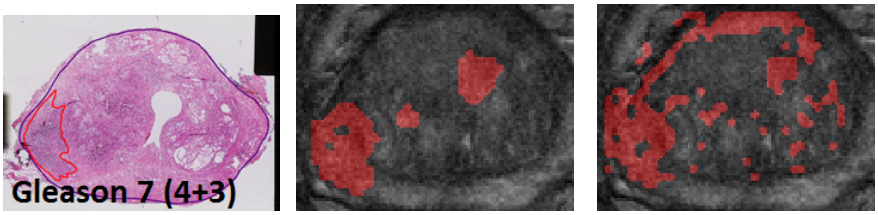

Fig. 1: From left to right: pathology samples, identification results of proposed method (6 texture atoms), identification results for [4].

elevated PSA require a follow-up transrectal ultrasound (TRUS) guided biopsy to assess malignancy. Recent studies [2] [13] indicate that the PSA test has a high risk of overdiagnosis, with an estimated 50% of screened men being diagnosed with prostate cancer. This oversensitivity results in expensive and painful prostate biopsies, which cause discomfort, possible sexual dysfunction, and may result in increased hospital admission rates due to infectious complications [10]. The challenge diagnosticians face is how to improve prostate cancer diagnosis by reducing the overdiagnosis caused by conventional screening methods while still maintaining a high sensitivity.

Current imaging-based cancer screening methods (such as the use of magnetic resonance imaging or MRI) require extensive interpretation by an experienced medical professional. One notable challenge is the variability between diagnosticians ("inter-observer variability") and the variability of a single diagnostician over multiple sittings ("intra-observer variability") when evaluating features using multi-parametric MRI (i.e. different MRI modalities) [7]. The European Society of Urogenital Radiology (ESUR) recently introduced PI-RADS, or the Prostate Imaging - Reporting And Diagnosis System [3]. PI-RADS is a set of guidelines for interpreting multiple MRI images, and aims to raise the consistency between diagnosticians through a common set of criteria.

Despite PI-RADS and further development to standardize the interpretation of multi-parametric MRI images [11], there is still a level of subjectiveness that can lead to inconsistent diagnosis. Notable challenges include noise in MR images, variability between different MRI modalities, weak contrast, and non-homogeneous texture patterns, making it difficult for diagnosticians to identify tumour candidates. Computer-aided cancer detection methods are being developed to help the physicians with the process.

One specific area of research is the identification of suspicious regions to aid physicians with performing a more efficient and accurate diagnosis. The current method for identifying suspicious regions is to threshold apparent diffusion coefficient (ADC) maps, as low ADC values are associated with tumorous tissue [6]. Cameron *et al.* [4] proposed a threshold-based approach where tissue associated with ADC values within a threshold range are automatically identified as suspicious. However, this method depends on fixed thresholds, making it susceptible to noisy MR images and ADC variations across different sets of multi-parametric MRI data.

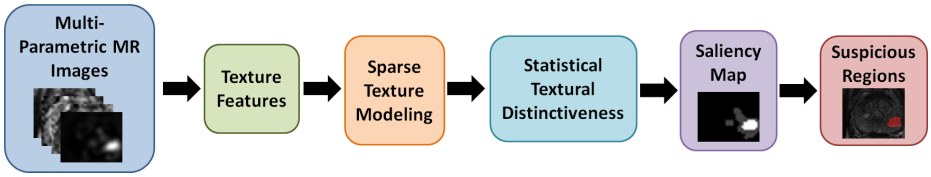

Fig. 2: Proposed framework for identifying suspicious regions using prostate multi-parametric MRI. Unique texture features extracted from different MRI modalities are used to learn a sparse texture model, and suspicious regions are identified via a statistical textural distinctiveness-based saliency map.

To facilitate a more reliable diagnosis, a novel method for identifying suspicious regions indicative of potential prostate cancer using texture-based saliency in multi-parametric MR images is proposed. The proposed method uses unique texture information from each MRI modality to learn a sparse texture model, and better characterize suspicious tissue within a patient's MRI data.

2 Methods

A novel method is proposed for identifying suspicious regions to better aid physicians with performing more efficient and accurate diagnoses. The proposed method uses multi-parametric MR images and incorporates cross-modality texture features to better identify suspicious regions via statistical textural distinctiveness. Figure 2 shows the general algorithmic framework developed.

2.1 Region-based textural representations

Region-based textural representations are used to allow for the characterization of texture features indicative of suspicious regions in prostate MR images. For region-based textural representations, we incorporate the feature set proposed by Khalvati *et al.* [8], which consists of sets of 19 low-level texture features extracted each from T2-weighted (T2w) images, apparent diffusion coefficient (ADC) maps, computed high-b diffusion-weighted imaging (CHB-DWI) data, and correlated diffusion imaging (CDI) data, to better capture healthy and cancerous tissue characteristics. These MRI modalities were selected based on their potential to separate cancerous from healthy prostate tissue.

The sets of texture features are combined into a single textural representation $h(x)$, and a compact version of the textural representation is produced using principal component analysis (PCA). A compact textural representation $t(x)$ is produced using the u principal components of $h(x)$ with the highest variance:

$$t(x) = \langle \Phi_i(h(x)) | 1 \leq i \leq u \rangle \tag{1}$$

where Φ_i is the i^{th} principal component of $h(x)$. While u can be selected based on variance compactness, u components of $h(x)$ were selected to represent 90% of the variance of all the textural representations as determined through extensive empirical testing.

2.2 Sparse texture model

To characterize healthy and suspicious tissue for a patient, a sparse texture model is learned using the extracted multi-parametric MRI texture features [8]. The sparse texture model incorporates unique texture features from each MRI modality to learn tissue characteristics via cross-modality texture information. Thus, the sparse texture model can better identify healthy and suspicious tissue.

Using a subset of $t(x)$ as training data, a global texture model is defined to represent the heterogeneous characteristics of healthy and suspicious prostate tissue. As global texture modelling is computationally expensive, we generalize an MRI slice as being composed of a set of regions where a particular texture pattern is repeated over a given area. In addition, the number of areas with unique texture patterns is assumed to be much fewer than the number of individual voxels in the training data.

Using this generalization, we can establish a textural sparsity assumption, and the global textural characteristics of prostate tissue can be well-represented using a small set of distinctive local textural representations. This allows for the use of a sparse texture model, defined as a set of m representative texture atoms:

$$T^r = \{t_i^r | 1 \leq i \leq m\} \tag{2}$$

The sparse texture model used in the proposed method is a set of representative texture atoms corresponding to healthy or suspicious tissue, where each texture atom represents the mean and covariance (i.e., $t_i^r = \underline{\mu}_i, \Sigma_i$) of a particular texture pattern characteristic of healthy or suspicious tissue. The representative atoms in the sparse texture model are learned via expectation maximization [1].

2.3 Statistical textural distinctiveness

Suspicious regions in prostate MRI data can be characterized as areas that are highly unique and texturally distinct. Using the concept of statistical textural distinctiveness [12], we quantify the distinctiveness of texture patterns and uncover the underlying saliency by using the statistical relationship between texture patterns across different MRI modalities.

To define statistical textural distinctiveness between two representative texture atoms (denoted as t_i^r and t_j^r) in the sparse texture model, we use Kullback-Leibler (KL) divergence [9] to measure the statistical difference between the representative texture atoms in the sparse texture model:

$$\beta_{i,j} = \log \frac{|\Sigma_j|}{|\Sigma_i|} - u + trace(\Sigma_j^{-1}\Sigma_i) + \frac{(\underline{\mu}_j - \underline{\mu}_i)^T \Sigma_j^{-1} (\underline{\mu}_j - \underline{\mu}_i)}{2} \tag{3}$$

where u is the number of PCA components selected, $\underline{\mu}_i$ and $\underline{\mu}_j$ represent the mean of t_i^r and t_j^r, respectively, and Σ_i and Σ_j represent the covariance of t_i^r and t_j^r, respectively. Thus, the distinctiveness metric $\beta_{i,j}$ increases as the texture patterns become more distinct from one another.

2.4 Suspicious region detection via saliency map computation

As the majority of prostate tissue is considered to be healthy, salient regions can be interpreted as suspicious due to the uniqueness and statistical occurrence of the corresponding cross-modality texture characteristics. Given a subset of compact texture features used for testing (denoted as $t(x)_Z$), the saliency map for a given MRI image can be computed using the previously determined statistical textural distinctiveness graphical model. The saliency α_i is defined as:

$$\alpha_i = \sum_{j=1}^{m} \beta_{i,j} P(t_i^r | t(x)_Z) \tag{4}$$

where $P(t_i^r|Z)$ is the occurrence probability of t_i^r in $t(x)_Z$.

For S_i being the set of texture representations that corresponds to saliency α_i, voxels belonging to salient representative texture atoms S_i (i.e., $\alpha_i > \frac{\alpha_{max}}{2}$) are classified as regions of suspicious tissue, with all other voxels classified as healthy tissue. That is, each voxel x in a given MRI image is assigned a label y:

$$y = \begin{cases} 1 & x \in S_i, \alpha_i > \frac{\alpha_{max}}{2} \\ 0 & otherwise \end{cases} \tag{5}$$

3 Results

3.1 Experimental Setup

The performance of the proposed method was evaluated using the MRI data of 13 patients acquired using a Philips Achieva 3.0T machine at Sunnybrook Health Sciences Centre, Toronto, Ontario, Canada. The resolution of the signal acquisitions ranged from 1.36 mm x 1.36 mm to 1.67 mm x 1.67 mm, with a median of 1.56 mm x 1.56 mm. Institutional research ethics board approval and patient informed consent for this study was obtained at Sunnybrook Health Sciences Centre. The patients' ages ranged from 53 to 75. The data set includes segmentation information to isolate the prostate, and ground truth data for tumour size and location. All images were reviewed and marked as healthy and cancerous tissue by a radiologist with 18 and 13 years of experience interpreting body and prostate MRI, respectively.

Each patient dataset had corresponding T2w images, ADC maps, CHB-DWI data, and CDI data. Using the radiologist contour of the prostate, a rectangle cropped around the prostate gland was selected as the region of interest (ROI) for each MRI slice. The performance of each method was evaluated using leave-one-patient-out cross-validation. A subset of the training texture features were randomly selected and used to train the classifier, and the voxels in a single MRI slice were classified as either healthy or cancerous tissue and assigned the saliency value of the nearest texture atom.

In addition, the number of texture atoms used to compute the spare texture model (as described in Subsection 2.2) was varied to determine the optimal number of representative texture atoms for identifying suspicious regions in prostate

MR images. The ADC-based method was compared against the proposed texture distinctiveness method (TD) via sensitivity, specificity, and accuracy metrics.

$$\text{Sensitivity} = \frac{TP}{P} \qquad \text{Specificity} = \frac{TN}{N} \qquad \text{Accuracy} = \frac{TN + TP}{N + P}$$

where the performance of each method was quantified by the metrics' closeness to one. TP is the number of voxels in the intersection of the identified cancerous tissue and the radiologist's tissue segmentation, TN is the number of voxels not in the identified tissue that are also not in the radiologist's segmentation, N is the number of voxels not in the radiologist segmented tissue and P is the number of voxels in the radiologist segmented tissue.

3.2 Experimental Results

The proposed textural distinctiveness method (TD) was evaluated using both four-atom and six-atom sparse texture models. Table 1 shows the performance metrics for the ADC-based method [4] and the proposed method. The testing data contained 52 tumours (as identified by an experienced radiologist) across the slices from 13 different patients.

Table 1: Comparison of TD (trained with both 4 and 6 texture atoms) with ADC-based method [4]. TD has similar sensitivity values as the ADC-based method, and improved specificity and accuracy values.

	Sensitivity	**Specificity**	**Accuracy**
ADC-based method [4]	0.7911	0.7107	0.7115
TD (4 texture atoms)	0.8088	0.8285	0.8283
TD (6 texture atoms)	0.8103	0.8303	0.8301

As seen in Table 1, the proposed TD method outperforms the ADC-based method [4] in terms of sensitivity, specificity, and accuracy. While there is only a relatively small increase in sensitivity (approximately 1.5%), TD shows an increase of at least 10% in specificity and accuracy relative to the ADC-based method. This is especially beneficial, as a low specificity negatively impacts a diagnostician's ability to perform quick and accurate assessments of MRI data. By increasing specificity, TD minimizes the number of wrongly detected regions that contain no tumour candidates. This is important for procedures such as radical prostatectomy where an extremely high specificity rate is required.

Figure 3 shows the suspicious regions detected using the ADC-based method [4] and the proposed TD method using four and six representative texture atoms. While all methods identify the cancerous regions as suspicious, the ADC-based method in particular has a tendency to be over-sensitive and often identifies a large portion of the prostate tissue as suspicious. A visual inspection of the identified suspicious regions shows that TD consistently produces spatially compact and useful regions regardless of the number of texture atoms.

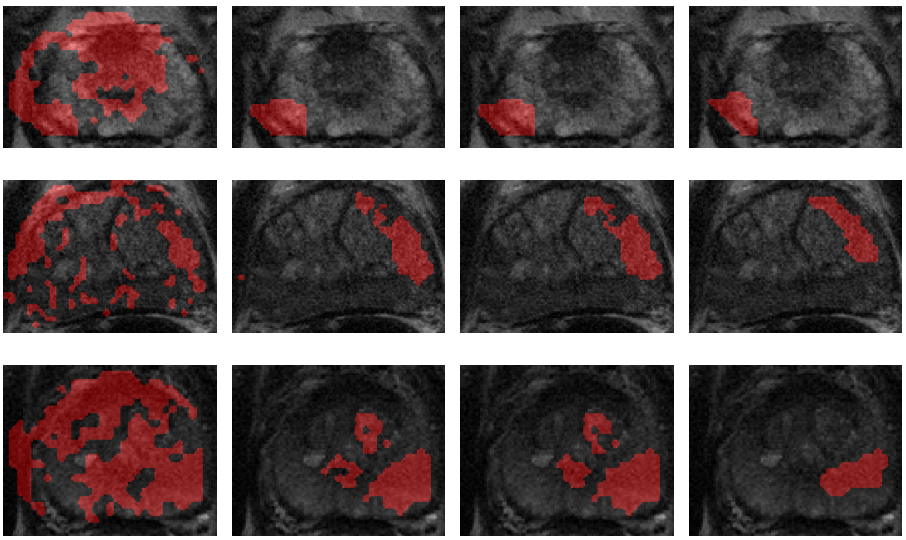

(a) (b) (c) (d)

Fig. 3: Visual comparison of identified suspicious regions (shown in red) between (a) ADC-based method [4], (b) TD using four texture atoms, (c) TD using six texture atoms, and (d) radiologist segmented regions.

4 Conclusion

A novel method was proposed to aid physicians in efficiently and accurately diagnosing patients via the identification of suspicious regions in prostate MR images. We extracted unique textural information from different MRI modalities, and used a sparse texture model to learn tissue texture characteristics. As the majority of prostate tissue is considered to be healthy, texturally distinct regions can be interpreted as suspicious due to the uniqueness and statistical occurrence of the corresponding cross-modality texture characteristics.

The proposed statistical textural distinctiveness approach (using four-atom and six-atom sparse texture models) was evaluated against the ADC-based method [4]. In both cases, statistical textural distinctiveness has higher sensitivity, specificity, and accuracy values than the state-of-art ADC-based method. In additional, statistical textural distinctiveness also identifies suspicious regions on a per patient basis, rather than relying on a fixed ADC value characteristic of typical cancerous tissue (as is the case with the ADC-based threshold method). Thus, statistical textural distinctiveness shows potential for more flexible and visually meaningful identification of suspicious tumour regions.

Future work includes the further investigation of additional MRI modalities, and the use of spatial consistency to enforce more compact identified suspicious areas. Applications include identifying suspicious regions for clinicians to better stream-line a patient's diagnosis, and automatically identifying regions of interest for computer-aided tumour detection methods.

References

1. Aitkin, M., Rubin, D.B.: Estimation and hypothesis testing in finite mixture models. Journal of the Royal Statistical Society. Series B (Methodological) pp. 67–75 (1985)
2. Andriole, G.L., Crawford, E.D., Grubb, R.L., Buys, S.S., Chia, D., Church, T.R., Fouad, M.N., Gelmann, E.P., Kvale, P.a., Reding, D.J., Weissfeld, J.L., Yokochi, L.a., O'Brien, B., Clapp, J.D., Rathmell, J.M., Riley, T.L., Hayes, R.B., Kramer, B.S., Izmirlian, G., Miller, A.B., Pinsky, P.F., Prorok, P.C., Gohagan, J.K., Berg, C.D.: Mortality results from a randomized prostate-cancer screening trial. The New England journal of medicine 360(13), 1310–9 (Mar 2009)
3. Barentsz, J.O., Richenberg, J., Clements, R., Choyke, P., Verma, S., Villeirs, G., Rouviere, O., Logager, V., Fütterer, J.J.: ESUR prostate MR guidelines 2012. European radiology 22(4), 746–57 (Apr 2012)
4. Cameron, A., Modhafar, A., Khalvati, F., Lui, D., Shafiee, M.J., Wong, A., Haider, M.: Multiparametric MRI Prostate Cancer Analysis via a Hybrid Morphological-Textural Model. In: Engineering in Medicine and Biology Society, 2014 36th Annual International Conference of the IEEE. pp. 3357–3360 (2014)
5. Canadian Cancer Society: Prostate cancer statistics (2014)
6. Haider, M.A., van der Kwast, T.H., Tanguay, J., Evans, A.J., Hashmi, A.T., Lockwood, G., Trachtenberg, J.: Combined T2-weighted and diffusion-weighted MRI for localization of prostate cancer. AJR. American Journal of Roentgenology 189(2), 323–8 (Aug 2007)
7. Khalvati, F.: Automated consensus contour building for prostate MRI. 2014 36th Annual International Conference of the IEEE Engineering in Medicine and Biology Society pp. 5534–5537 (Aug 2014)
8. Khalvati, F., Modhafar, A., Cameron, A., Wong, A., Haider, M.A.: A multiparametric diffusion magnetic resonance imaging texture feature model for prostate cancer analysis. In: MICCAI 2014 Workshop on Computational Diffusion MRI. pp. 1–10. Medical Image Computing and Computer Assisted Intervention (2014)
9. Kullback, S., Leibler, R.A.: On information and sufficiency. The annals of mathematical statistics pp. 79–86 (1951)
10. Loeb, S., Vellekoop, A., Ahmed, H.U., Catto, J., Emberton, M., Nam, R., Rosario, D.J., Scattoni, V., Lotan, Y.: Systematic review of complications of prostate biopsy. European urology 64(6), 876–92 (Dec 2013)
11. Röthke, M., Blondin, D., Schlemmer, H.P., Franiel, T.: [PI-RADS classification: structured reporting for MRI of the prostate]. RöFo : Fortschritte auf dem Gebiete der Röntgenstrahlen und der Nuklearmedizin 185(3), 253–61 (Mar 2013)
12. Scharfenberger, C., Wong, A., Fergani, K., Zelek, J.S., Clausi, D.A.: Statistical Textural Distinctiveness for Salient Region Detection in Natural Images. In: Computer Vision and Pattern Recognition (CVPR), 2013 IEEE Conference on. pp. 979–986 (2013)
13. Schröder, F.H., Hugosson, J., Roobol, M.J., Tammela, T.L.J., Ciatto, S., Nelen, V., Kwiatkowski, M., Lujan, M., Lilja, H., Zappa, M., Denis, L.J., Recker, F., Berenguer, A., Määttänen, L., Bangma, C.H., Aus, G., Villers, A., Rebillard, X., van der Kwast, T., Blijenberg, B.G., Moss, S.M., de Koning, H.J., Auvinen, A.: Screening and prostate-cancer mortality in a randomized European study. The New England journal of medicine 360(13), 1320–8 (Mar 2009)